ISSN 1392 - 1207. MECHANIKA. 2011. 17(1): 21-29

Model of radial deformations of protector of vehicle tire

J. Sapragonas*, A. Dargužis**
**Kaunas University of Technology, Kęstučio 27, 44312 Kaunas, Lithuania, E-mail: jonas.sapragonas@ktu.lt*
***Kaunas University of Technology, Kęstučio 27, 44312 Kaunas, Lithuania, E-mail: andrius.darguzis@ktu.lt*

crossref http://dx.doi.org/10.5755/j01.mech.17.1.199

1. Introduction

For stability of a vehicle, the problem of interacttion of tire with road is one of the most complicated tasks. For analysis of the tire and road contact, it is necessary to evaluate tire deflection features. It is rather complex task due to some uncertainty of tire operational conditions and sophisticated structure of the tire itself. Problem's complexity is emphasized by the absence of common opinion about tire shape till now. The geometric tire model was described by toroid [1] in earlier works, and the band model was used later [2]. Modern studies of contact zones of broad tires [3] would conform more to the ring model of limited flexibility.

Variation of dimensional position of a wheel due to kinematic properties of the suspension [4] causes tire deflection in transversal, longitudinal and vertical directions, and protector angular deflections with respect to the plane of the wheel (Fig. 1). Increasing loadings cause deflection of elements of suspensions and steering-wheel mechanism, what can change the tire dimensional position.

For the formation of corrected vehicle stability models, tire deflection characteristics are needed [5]. Experimental data are supplied rarely and they are typical to the concrete tire.

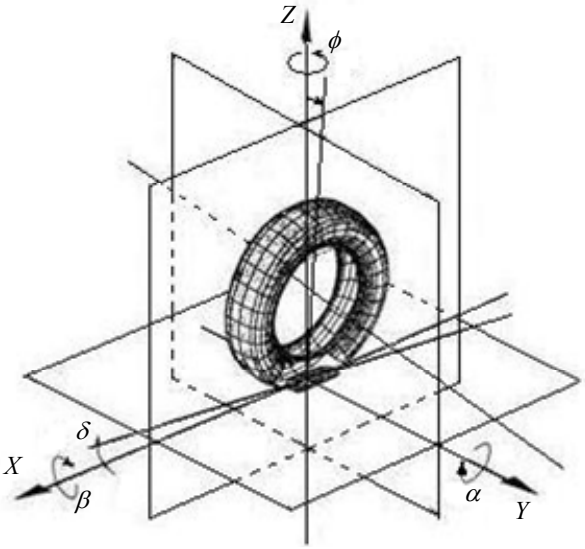

Fig. 1 Coordinate of 3D wheel model

Tire characteristics need to be corrected when solving tasks of dynamics of the tire itself. Operation analysis of high speed vehicles suspensions [6] demonstrates that there appears an additional vibration source, which is related to natural tire vibrations by the authors of the works quoted. For this purpose in vehicle's quarter model (Fig. 2) deformations of an additional element – protector are needed to be evaluated individually.

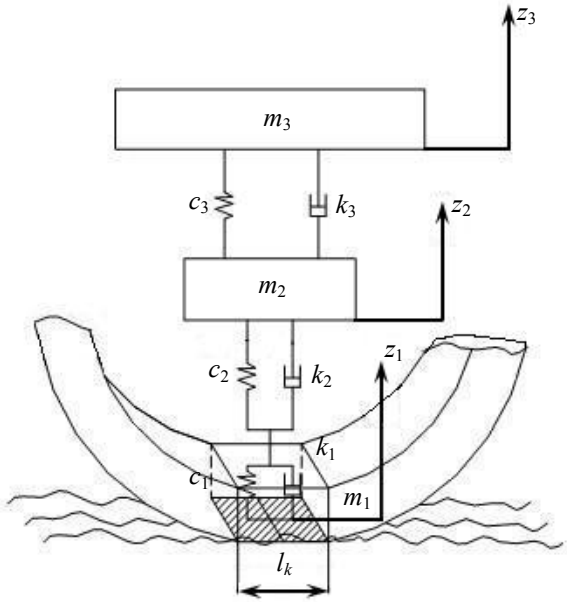

Fig. 2 Vehicle quarter model: L_k – length of the tire and road contact; m_1, c_1 and k_1 – mass, rigidity and damping factor of part of the tire protector; c_2, k_2 – tire rigidity and damping factor; c_3, k_3 – suspension rigidity and damping factor of a shock absorber; m_2 – unsprung mass; m_3 – sprung mass

Purpose of this work is to compare deformability of tires of different types, thus permitting to use for modeling tire deflection characteristics of the same tire group. Common regularities of composite mechanics were used in the work and possibilities of the application of some assumptions were analyzed.

2. Subjects of investigation

Modern tire has complex structure (Fig. 3). For the analysis of tire deflection features, structure of the tire is simplified, dividing the tire into a ring and sides. The ring, consisting of protector, breaker, plies of cord and internal ply, is described as layered structure [1, 2]. It is assumed in the simpler models, that its band is absolutely rigid to stress but ideally flexible, though investigations of its features [7] confirm, that the band is not absolutely flexible. The sides in many models are described as a band of cord fiber or a band, in which rubber is used just for ensuring tightness [1]. Mechanical features of rubber were not taken into account, so the sides are calculated as single cord threads. Such model is applicable for the description of static tire deflection, when mass of the tire elements, their inertia moments and damping elements may not be evaluated. With these assumptions applied, deformations

of the tire elements could be expressed by elasticity characteristics of their materials. Other tire elements are simplified too. Experience of the application of computational models shows that these models do not specify tire characteristics in full, and results are to be corrected according to experimental data.

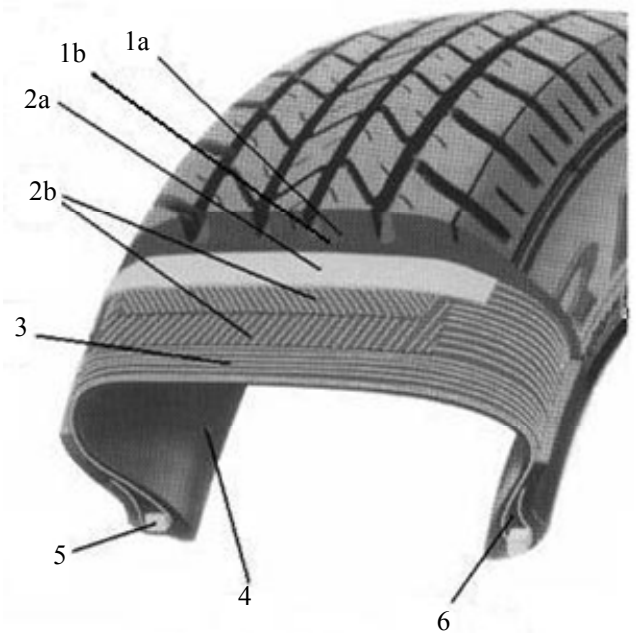

Fig. 3 Elements of the radial tire: *1a* – protector part with a pattern, *1b* – continuous protector part, *2b* – breaker, *2b* – breaker, *3* – radial ply, *4* – inner sealing layer, *5* – fixing ring, *6* – sidewall belts

The radial tires of three types with different structure were analyzed in the work: tires of a motorcar (175/70R13; 195/50R15), light truck (185/75 R14C) and lorry (12.00R20). Characteristics of the tire elements are presented in Table 1.

3. Investigations of protector deformations

Influence of the ring and side on tire deformation properties is analyzed in work [2] in more details. Deformation characteristics of separate tire elements in this work are defined after disintegration of them into monolayers, consisting of rubber or rubber, reinforced by fiber oriented to single–direction. Investigations done on interaction of the tire and the road [4, 6] confirmed, that while evaluating tire compensation function it is necessary to evaluate deformation features of the band, with entering an additional element into quarter model of the vehicle (Fig. 2). In order to determine deformation features of this element the tire is divided by elements into a band of ring shape, consisting of a protector, breaker, cord and protective layers, connected flexibly with toroidal sides, composed of rubber reinforced with cord. The protector model consists of two layers: ribbed and not ribbed ones, connected consequently.

3.1. Protector deformations under compression

Protector part with a pattern and continuous protector part of the protector are isotropic materials and conditionally can be analyzed as a material close to the rubber by their features. As modeling their behavior, we used equations applied for rubber parts, evaluating, that Poisson's ratio is $\nu = 0.5$.

Table 1

Data of tire constitutive parts

	Tire	Tire elements	
		thickness, mm	angle of fiber, °
A	175/70R13	δ_{1a}=8.0	–
		δ_{1b}=2.1	–
	Breaker 3 layers	δ_2=2.7	θ_2=20°
	Cord 1 layer	δ_3=0.9	θ_3=90°
		δ_4=0.9	–
B	195/50R15	δ_{1a}=8.1	–
		δ_{1b}=2.1	–
	Breaker 2 layers	δ_2=3.6	θ_2=20°
	Cord 2 layers	δ_3=0.9	θ_3=90°
		δ_4=1.0	–
C	185/75R14C	δ_{1a}=12.0	–
		δ_{1b}=3.0	–
	Breaker 2 layers	δ_2=3.2	θ_2=20°
	Cord 2 layers	δ_3=1.8	θ_3=90°
		δ_4=1.0	–
D	12.00R20	δ_{1a}=17.8	
		δ_{1b}=3.9	
	Breaker 4 layers	δ_2=6.4	θ_2=20°
	Cord 6 layers	δ_3=7.2	θ_3=90°
		δ_4=1.0	–

Note: θ – angle of cord with respect to rolling direction, δ_{1a} – protector part with a pattern, δ_{1b} – continuous protector part, δ_2 – breaker, δ_3 – cord, δ_4 – sealing layer.

In the works, analyzing pneumatic tire, rather wide limits of rubber elasticity modulus $E_r = 2 - 20$ MPa are prescribed [1, 2]. For the analysis of simplified car tire model in the work [2] $E_r = 18$ MPa there was used, what is related to objective of reaching adequate deformation characteristics for the whole tire. In order to correct initial characteristics, an experiment was performed to define trodden down band of a truck tire, coincident to protector of the tire 12.00R20, with wide part 313 mm. Height of the ribbed part of the protector is $\delta_{1a} = 17.8$ mm, and height of not ribbed one is $\delta_{1b} = 3.9$ mm. Under compression the protector was loaded up to the loading, corresponding by pressure to nominal radial loading R_{znom} for tire of type 12.00R20. The universal extension – compression machine Amsler was used for the investigation. Deformations were estimated by an indicator of 0.01 mm accuracy measuring variation of the distances between machine plates. Friction between polished machine steel plates and the protector was reduced by lubrication.

The obtained experimental results are generalized in Fig. 4. Dependence of loading–deformation achieved was very close to linear (correlation coefficient $r_{xy} = 0.947$), what confirmed the possibility of application of linear elastic material description as investigating protector deformations. According to experimental results protector elasticity modulus defined is 7.84 MPa, with the evaluation of ribbed protector part by filling coefficient,

we would get $E_r = 6.16$ MPa, that is considerably less, than in the work [2]. Besides, it is necessary to take into account, that softer rubber is used for motorcar tires.

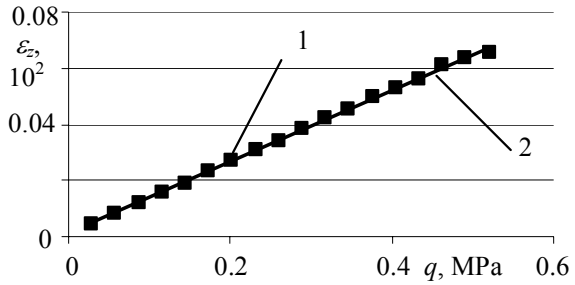

Fig. 4 Protector band deformations (*1* – experimental points, *2* – generalized line)

In order to correct the results obtained, operational conditions of the protector were examined in greater detail.

3.2. Porous composite model

The simplest model evaluates filling of the ribbed part

$$E = k_u E_r \tag{1}$$

where k_u is protector filling coefficient, and $k_u = A_i / A_p$; A_i is area of continuous part in the selected by pattern recurrence protector part; A_p is area of protector part selected; E_r is elasticity modulus of protector rubber.

As protector pattern in different its parts is not the same, filling coefficient for every protector band is calculated individually. Then, equivalent elasticity modulus of the protector is equal to

$$E_1 = E_g \frac{\sum k_{ui} k_{bi}}{1 - k_a \left(1 - \sum k_{ui} k_{bi}\right)} \tag{2}$$

where $k_a = \delta_{1a} / \delta_1$; $\delta_1 = \delta_{1a} + \delta_{1b}$; k_{bi} is *i*-th part of band width in the protector width.

Elasticity modulus of the whole protector is calculated from equation

$$\frac{1}{E_1} = \left(\frac{\delta_{1a}}{E_{1a}} + \frac{\delta_{1b}}{E_{1b}}\right)\frac{1}{\delta_1} \tag{3}$$

Results, obtained for different tires, are presented in Table 2.

Table 2

Elasticity modulus of the protector, obtained with evaluation of filling

Tire type	Ribbed part E_{1a}, MPa	Continuous part E_{1b}, MPa	Protector E_1, MPa
A	5.72	7.84	6.16
B	5.88	7.84	6.22
C	7.08	7.84	6.51
D	5.33	7.84	5.37

This model reflects operational conditions of the protector incorrectly. Deformations of ribbed part of the protector may be restricted by contact with road, continuous breaker. Besides, deformations of ribbed part of the protector are running not exactly by ideal compression conditions, because with restriction of ends deformations, element's form changes.

3.3. Model of rubber prism under compression

Deformations of ribbed part of the protector may be evaluated by calculation methods of rubber prism shock absorbers. In this way, protector element is imagined as rubber prism, deformed with more or less constricted end deformations, subject to conditions. For this purpose deformation equations of rubber shock absorbers are used in work [8]. If deformations of both ends of rubber shock absorber of prism shape are constricted, relation between loading and deformations is expressed by the equation

$$R_z = \frac{1}{3}\beta E A\left(\frac{1}{\lambda^2} - \lambda\right) \tag{4}$$

where $\lambda = 1 - \frac{\Delta\delta}{\delta}$, $\beta = \frac{4}{3}\left(1 + \eta^2 - \eta\right)\left(1 - \frac{2}{\alpha\delta} th \frac{\alpha\delta}{2}\right)^{-1}$; A is area of prism base: δ is height of the prism; $\Delta\delta$ is deformations of the prism; α and η are parameters of form change under compression.

As α and η are interconnected, system of equations is proposed in the work [8], obtained from energy minimum condition

$$\alpha^2 = \frac{1}{b^2}\frac{48\left(1 + \eta^2 - \eta\right)}{\eta^2\left(\frac{a}{b}\right) + (1 - \eta)^2} \tag{5}$$

$$\frac{\alpha\delta - 2\,th\frac{\alpha\delta}{2}}{\alpha\delta\left(th^2\frac{\alpha\delta}{2} - 1\right) + 2\,th\frac{\alpha\delta}{2}} = \frac{1}{2} + \frac{1 + \eta^2 - \eta}{1 - 2\eta} \cdot \frac{\eta\left(\frac{a}{b}\right)^2 + \eta - 1}{\eta^2\left(\frac{a}{b}\right)^2 + (1 - \eta)^2} \tag{6}$$

where *a* and *b* are dimensions of prism base.

Equations (5) and (6) were solved by approximation method.

Such model of ribbed part of the protector was applied in two cases: when end deformations are not constricted and when they are fully constricted. If deformations of shock absorber ends are not constricted, $\beta = 1$. With deformations constricted, rigidity of separate bands of ribbed part of the protector increases up to 4.5 times (Table 3).

The second model of protector deformations permits the influence of the evaluation of protector deformations constriction in circular (X) and radial (Y) directions on radial deformations in the case of absolute constriction of deformations. Under real conditions the constrictions of

deformations of ribbed part of the protector ends are not absolute. In contact with road deformations of ribbed part of the protector are constricted by friction forces between the road and the tire, deformations of not ribbed part of the protector are constricted by layers of breaker and cord, reinforced with fiber. If breaker layers are not rigid (especially in transversal direction), conditions of deformations of ribbed part of the protector are closer to the ones of shock absorber with freely deforming ends, and if the deformation is constricted, we will have to evaluate the deformation constriction.

Table 3

Values of stiffening coefficient of protector elements for individual protector bands

Tire type	Band number	Length a, mm	Width b, mm	β for band
A	1	39	29	3.83
	2	32	29.6	3.67
B	1	37	29	3.75
	2	31	29	3.67
	3	239	24	4.58
C	1	33	20	2.62
	2	36	18	2.08
D	1	116	42	3.33
	2	90	41	3.17

In order to estimate influence of the latter constriction more exactly, deformation characteristics of tire abstracted ring, consisting of protector, breaker, cord and protective layer (Fig. 3), were determined.

3.4. Influence of deformations constriction of the protector on stiffness

Deformation characteristics of separate tire elements were defined dividing them into monolayers (Table 1.), consisting of rubber or rubber, reinforced with single-oriented fiber.

Band of the tire 175/70R13 designed for motorcars by Nokian company was simulated. Its structure in more details is presented in Table 4.

Elasticity characteristics of a mono-ayer are defined according to equations of composite mechanics [9, 10]

$$E_{c1} = E_f \varphi_f + E_m (1 - \varphi_f) \tag{7}$$

$$E_{c2} = E_m \left((1 - \varphi_f) + \frac{E_m}{E_{f2}} \varphi_f \right)^{-1} \tag{8}$$

$$G_{c12} = G_m \left((1 - \varphi_f) + \frac{G_m}{G_{f12}} \varphi_f \right)^{-1} G_f \tag{9}$$

$$\nu_{c12} = \varphi_f \nu_{f12} + \varphi_m \nu_m \tag{10}$$

where E_c, G_c, E_m, G_m are elasticity and shear modulus of composite matrix and filling; φ_f and φ_m are volume parts of filling and matrix; ν_f and ν_m are Poisson's ratios of composite, filling, and matrix; *1* – direction along fiber; *2* – direction across fiber.

Table 4

Dividing into layers of tire 175/70R13 bands

Layer No.	Layer description	Thickness, mm
1	Protector with pattern	2.9
2	Protector without pattern	2.1
3	Nylon – rubber	0.8
4	Steel – rubber	0.9
5	Rubber	0.9
6	Steel – rubber	0.9
7	Viscose – rubber	0.9
8	Sealing layer	0.9

The given equations should be corrected, so as they do not evaluate the difference of Poisson's ratios of components [10]. In our case, for pair – rubber ($\nu = 0.5$) – steel ($\nu = 0.25$), having even the largest difference of Poisson's ratios due to a big difference of elasticity modulus of the components, the correction does not change the value of composite elasticity modulus, so while defining characteristics of the layers, differences of Poisson's ratios are not taken into account.

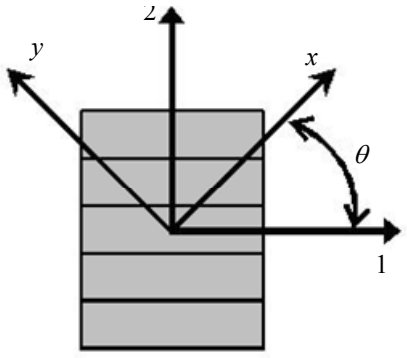

Fig. 5 Element of layered composite

Features of the layers of cord and breaker in longitudinal and transversal directions are defined by using expressions of state of plane stress for anisotropic mono–layer [9, 2]: with the application to axes presented in Fig. 5

$$\begin{Bmatrix} \varepsilon_x \\ \varepsilon_y \\ \gamma_{xy} \end{Bmatrix} = [T'] \begin{Bmatrix} \frac{1}{E_1} & -\frac{\nu_{21}}{E_2} & 0 \\ -\frac{\nu_{21}}{E_2} & \frac{1}{E_2} & 0 \\ 0 & 0 & \frac{1}{G_{12}} \end{Bmatrix} [T] \begin{Bmatrix} \sigma_x \\ \sigma_y \\ \tau_{xy} \end{Bmatrix} \tag{11}$$

where $[T'] = \begin{bmatrix} c^2 & s^2 & cs \\ s^2 & c^2 & -cs \\ -2cs & 2cs & (c^2 - s^2) \end{bmatrix}$;

$[T] = \begin{bmatrix} c^2 & s^2 & -2sc \\ s^2 & c^2 & -2sc \\ sc & -sc & (c^2 - s^2) \end{bmatrix}$; $c = \cos\theta$, $s = \sin\theta$.

Elasticity modulus and Poisson's ratios of the components are taken from the works [1 - 3]. It was as-

sumed, that fiber of nylon and viscose is anisotropic, elasticity modulus along and across the fiber are different.

While investigating tire band structure, the problem of dividing into layers appeared. There is the rubber layer between separate bands of breaker, reinforced with steel wire. Therefore the band was examined additionally separating the rubber layer between the reinforced layers (Fig.6, a; Table 4) and using simplified separation into two layers (Fig.6, b).

While investigating deformation features of the whole band, the model used in layered composites was applied firstly. Theoretical elasticity modulus of the band, as the composite has been calculated with the evaluation of elasticity module of the layers connected in parallel (directions X and Y) or consequently (direction Z).

So as reinforcement angles of adjacent breaker layers differ just by a sign (+ 20° and – 20°), it was assumed, that shear forces appearing in these layers counterbalanced and were not transferred to other layers.

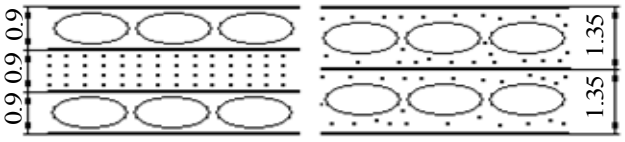

Fig. 6 Calculation schemes of breaker layers: a) with rubber layer excluded, b) with rubber layer not excluded

It was found out, that while understanding the large difference between elasticity modulus of reinforcement fiber and rubber, the rubber elasticity modulus does not have a considerable influence upon elasticity modulus of the layer in the direction of reinforcement. With the variation of elasticity modulus of the rubber in the range 2 - 20 MPa, band's elasticity modulus in direction Y (direction of cord fiber) varies by 3.7% only. The way of layers exclusion (a and b) in this case does not have any influence too. Herewith it was found out, that in the direction of breaker fiber (X) and in direction Z fiber's elasticity modulus depends more distinctly on the rubber elasticity modulus. Elasticity modulus in direction X depends on E_r less. With the variation of rubber elasticity modulus in the range 2 - 20 MPa, E_x differs by 3.7% for *a* model (Fig. 6, a) and by 3.5% for *b* model (Fig. 6, b). Especially distinct is the dependence of E_z: with E_r variation tenfold, E_z varies 9.97 of time (Fig. 7).

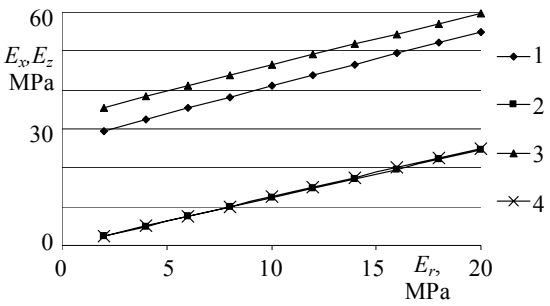

Fig. 7 Elasticity modulus of the tire band in directions X and Z: *1* – a model in direction X, *2* – a model in direction Z, *3* – b model in direction Z, *4* – b model in direction Z (a model – 8 layers, b model – 7 layers)

So as deformational features of the band in direction Z differ considerably from other authors' ones, an assumption was done, that more rigid cord and breaker layers might constrict deformations of the protector and with the state of constricted deformations, Poisson's ratio, close to 0.5, might have considerable influence on protector's deformation. Therefore protector deformation under compression was investigated additionally together with assumptions, reflecting interaction of separate layers in excluded tire band more correctly. For this purpose two cases were discussed. In the first case an assumption was applied, that when the band is deformed in direction Z, deformations of all layers in directions X and Y are the same

$$\varepsilon_{x1} = \varepsilon_{x2} = ... = \varepsilon_{xn}\,,\ \varepsilon_{y1} = \varepsilon_{y2} = ... = \varepsilon_{yn} \qquad (12)$$

Sum of unitary axial forces appearing in separate layers in directions X and Y is equal to 0

$$\left.\begin{aligned} &\delta_1\sigma_{x1} + \delta_{x2}\sigma_{x2} + ... + \delta_n\sigma_{xn} = 0 \\ &\delta_1\sigma_{y1} + \delta_{y2}\sigma_{y2} + ... + \delta_n\sigma_{yn} = 0 \\ &\sigma_{z1} = \sigma_{z2} = ... = \sigma_{zn} = \sigma_z = q \end{aligned}\right\} \qquad (13)$$

Numerical experiment has shown, that elasticity modulus of rubber in direction Z increases greatly, therefore elasticity modulus of the whole band in direction Z (Fig. 8) increases. Numerical experiment confirms, that the models, projecting an equal layers deformation, are especially sensitive to components with Poisson's ratio, close to 0.5. Conditional rubber elasticity modulus when structure of the layers matches the tire 175/70R13 subject to a layer is equal 86.3 MPa. Because of this reason the model with abstracted rubber interlayer predicts unreal big stiffness.

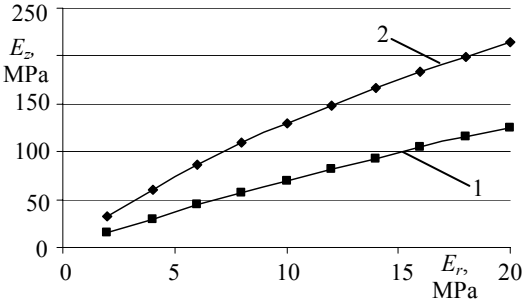

Fig. 8 Dependence of elasticity modulus of tire band on rubber elasticity modulus ($\sigma_z = 0.2$ MPa): *1* – 7 plies, *2* – 8 plies

In the second case we estimate friction between the protector and the road and assumed, that protector's deformation is constricted, till shear force appearing in directions X and Y does not exceed the friction force. So as a control experiment was intended, in computational model we assume, that friction forces are acting in another band side, too – in contact with the sealing layer. Numerical experiment confirmed that friction has an influence on value E_z (Fig. 9). With friction coefficient increasing, band stiffness in transversal direction increases quickly. Abstracted additional rubber layers have less influence in this case (Fig. 9).

In order to correct the results obtained, an attempt to deform a band cut out from the tire in direction Z was done. The experiment was performed with a band of tire 175/70R13 by Nokian company applied for the simulation.

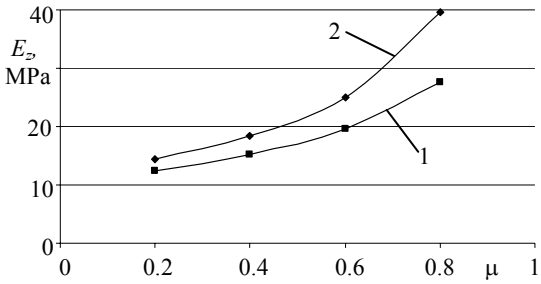

Fig. 9 Dependence of deformations of tire band on friction between contact plane and protector ($\sigma_z = 0.2$ MPa, $E_r = 6$ MPa): *1* – 7 plies, *2* – 8 plies

An universal tension-compression machine and equipment, used to investigate protector band, was applied for the research. Generalized experimental data are presented in Fig. 10.

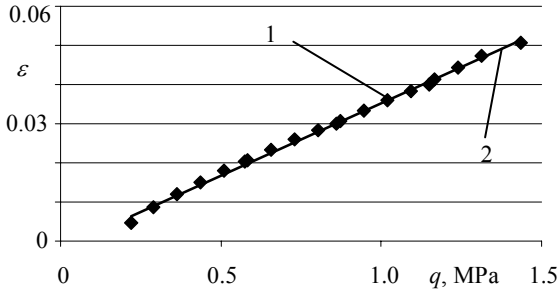

Fig. 10 Generalized experimental data: *1* – experimental data, *2* – linearized trendline

The experiment confirmed, that linear dependence of pressure and deformation remains till pressures, exceeding the range of operational pressures (tests were performed till $q = 1.5$ MPa). The calculated elasticity modulus of the whole band is equal 27 MPa, what corresponds to computational model of simplified structure (7 layers), evaluating friction between the plates and the band.

According to simulation data, with an assumption, that for rubber $E_r = 7.84$ MPa, calculated elasticity modulus of ribbed part of the protector is equal to 5.72 MPa, and one of not ribbed part is equal to 7.84 MPa. Cord is evaluated in the calculation of radial loadings in simplified tire models. Therefore breaker layers may be considered conditionally participating in radial deformation of the protector, as well. Thus by calculation expressions for layered composites with consequently located layers we would get:

$$\frac{1}{C^*_{prz}} = \frac{\delta_1}{C^*_{1z}} + \frac{\delta_2}{C^*_{2z}} + \frac{\delta_3}{C^*_{3z}} \qquad (14)$$

where C^*_i is a member of stiffness matrix with respect to deformations constriction.

Thus the member of stiffness matrix of tire protector tested C^*_z would be equal to 27 MPa.

For simulation of the real protector operation loadings and operational conditions of the protector should be corrected by approaching the computational model to real conditions.

4. Correction of protector loading

4.1. Comparative determination of pressure

It is rather complicated thing to compare the models investigated, because they present different characteristics – elasticity modulus E_1 or deformation $\Delta\delta$, corresponding to the value of radial loading R_z. To compare the results generalized characteristic, describing relation between loading and strain – stiffness C_1, was used

$$\Delta\delta = C_1 R_z \qquad (15)$$

where C_1 is protector stiffness, R_z is loading of radial tire.

For determination of value C_1 by the first or the second model, we have to evaluate the fact that area of the contact with road and volume of the deformed part of the protector depends on loading. For finding the area of contact with road, we used these assumptions:

- the contact with road is of elliptic shape, restricted by tire area and length of the contact with the road;
- layers under the protector are rigid enough, their length does not change with the tire being deformed;
- dependence of the tire radial deflection and radial loading are linear;
- pressure in the contact area distributes evenly.

The second and third assumptions permit finding out length of the contact with the road

$$L_k / 2 = r \arccos\left(\left(1 - C_R R_z\right)/ r\right) \qquad (16)$$

where C_R is radial stiffness of tire, r is free radius of tire (Table 5).

Table 5

Exploitational data of tires investigated

Exploitational data	A	B	C	D
Free radius *r*, mm	288	293	323	561
Static radius r_{st}, mm	262	267	288	520
Nominal loading $R_{z\,nom}$, N	4.7	4.7	8.3	36.8
Protector width *B*, mm	177	201	184	313

By expression of an ellipse area we get the contact area and comparative pressure in the contact:

$$q = 4R_z / \pi BL \qquad (17)$$

where B is width of the tire protector.

The assumptions permit finding pressure in the contact zone. Tire loading was calculated according to the tire nominal loading R_{znom} (Table 5). The pressure in the contact is calculated for loadings (0.25 – 1.25) R_{znom} For all tires investigated nonlinear $q(R_Z)$ dependence (Fig. 11)

was obtained. We notice, that tires operate in different pressure sections and operational conditions of the protector for motorcars and trucks differ by 1.5 - 1.7 time, the ones of motorcars and lorry – up to 3.2 times (Fig. 11). Therefore we compared protector's stiffness using not comparative pressure, but ratio $R_z^* = R_z / R_{znom}$.

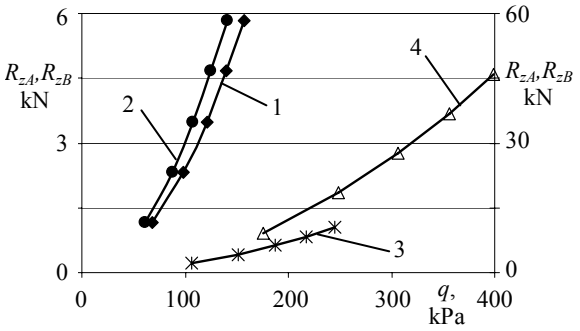

Fig. 11 Radial loadings and contact pressures of tires investigated: *1* – tire A, *2* – tire B, *3* – tire C, *4* – tire D

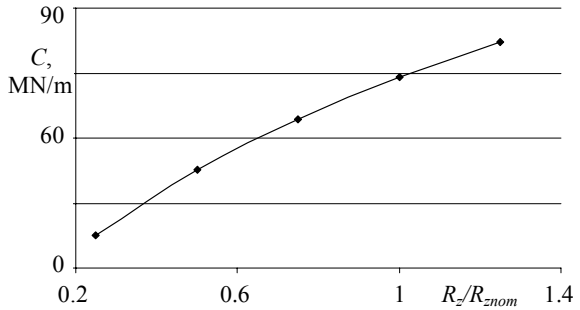

Fig. 12 Dependence of stiffness of ribbed part of the protector on relative radial loading for tire A

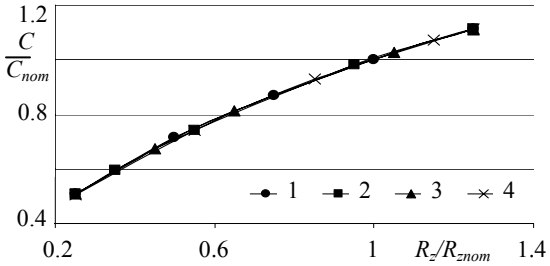

Fig. 13 Dependence of stiffness of ribbed part of the protector on relative radial loading for different tires: *1* – tire *A*, *2* – tire *B*, *3* – tire *C*, *4* – tire *D*

Nonlinear dependence $C_{1a}(R_Z)$ (Fig. 12) was noticed, which is related to nonlinear dependence of R_z and the length of contact with the road, from this follows nonlinear $q(R_Z)$ dependence, reducing protector's deformation in larger loadings zone. That is the particularity of tire contact with the road what explains that the tire type has no essential impact on the nature of dependence $C_{1a}(R_Z)$ (Fig. 13), as well.

Thickness of ribbed part has an influence on protector's stiffness. While evaluating the influence of this part by protector filling coefficient or by the model of rubber prism deformations, results differ not so much, if constrictions of the prisms ends are not taken into account.

The influence of protector's wear on its stiffness was defined by the model of short rubber prisms deformation. For the calculations of protector's stiffness, the influence of constriction of prism ends is not taken into account. For the calculation of protector's stiffness of the tire of A type protector's height is 8.1 mm for a new tire, 1.6 mm for worn one, besides, intermediate wear level (3.2 mm) is projected. Protector's wear changes the dependence $C - R_z$ very slightly (Fig. 14), but has considerable influence on the stiffness value itself. The influence is not monotonous – stiffness especially varies in the beginning of wear (Fig. 15). For the tires investigated wear of the protector may increase protector's stiffness for nominal loading up to 1.3 times.

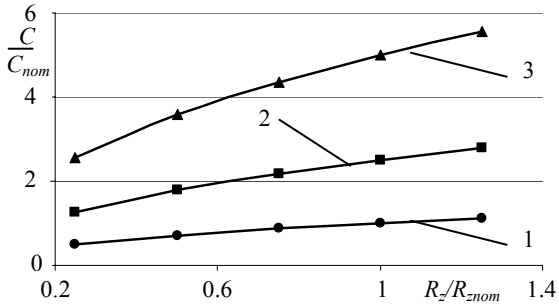

Fig. 14 Dependence of stiffness of ribbed part of the protector of tire A on protector's height: *1* – new tire, *2* – wear 50 %, *3* – wear out

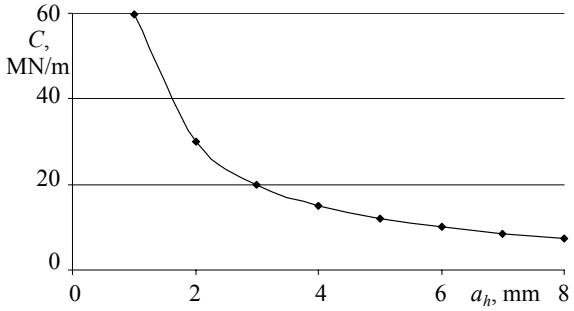

Fig. 15 Dependence of stiffness of the protector of tire A on wear

4.2. Model of protector interaction with road covering texture

The third deformation model of the protector was used in order to evaluate particularity of the tire interaction with road texture. The road texture is unevenness of road covering. For blacktop height of these inequalities is 1 - 5 mm [13 - 14]. An assumption was done, that the inequalities are bumps of semisphere shape located regularly (Fig. 16). This assumption permits modeling of interaction

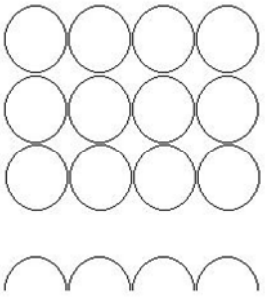

Fig. 16 Scheme of road unevenness

of a single bump with the protector with the assumption that a bump acts on continuous part of the protector. Coefficient of filling with spheres, required for recalculation of comparative pressure is equal to $\pi/4 = 0.785$. From geometric conditions it is found out, that gaps between the spheres will be filled when impact of a sphere into protector is equal to: $\Delta = 0.455r$, here r is radius of the sphere.

To investigate the interaction resolution of elastic deformations of the known sphere – plane contact was used. The interaction scheme is presented in Fig. 17. Shape inequality of semisphere with radius r, force F presses on protector, which is on rigid base. Therefore inequality squeezes in the protector by depth Δ. Dent radius is equal to c. Elastic resolution of such task is known [15]. Dent radius c is equal

$$c = 0.721\sqrt[3]{2Fr(k_1 + k_2)} \tag{18}$$

where $k_i = 1 - \nu_i^2 / E_i$; E_i, ν_i is elasticity modulus and Poisson's ratios of material of the sphere and plane ($E_1 = 18$ MPa, $\nu_1 = 0.5$, $E_2 = 6$ GPa, $\nu_2 = 0.3$).

The average pressure in contact

$$q_0 = 0.918\sqrt[3]{F/(2r(k_1 + k_2))}^2 \tag{19}$$

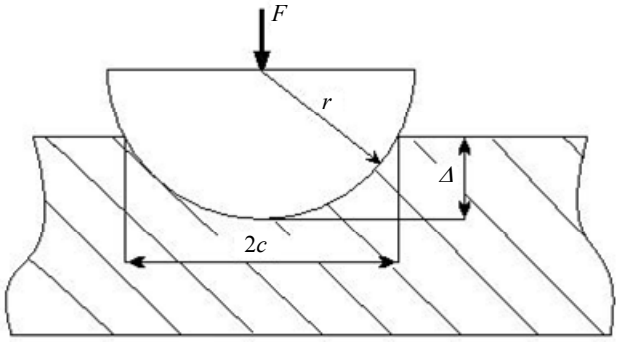

Fig. 17 Scheme of interaction of unevenness – protector

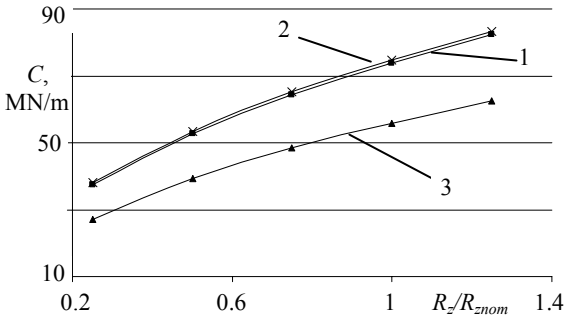

Fig. 18 Dependence of stiffness of ribbed part of the protector of the tire A on relative radial loading using different calculation models: *1* – model, *2* – model, *3* – model

Value F is selected such way, that pressure q, acting at tire and road contact when the tire is loaded with R_z, is equal to the average pressure in the contact sphere – protector q_0, with the evaluation of coefficient of filling with spheres in the contact. Taking into account, that according to elastic resolution:

$$\Delta = 0.825\sqrt[3]{\frac{F^2}{r}(k_1 + k_2)^2} \tag{20}$$

$$q_0 = \frac{F}{\pi c^2} \tag{21}$$

and with entering condition $q_0 = q$, we would get

$$\Delta = 5.552q^2 r(k_1 + k_2)^2 \tag{22}$$

Calculations confirm that condition $\Delta < 0.455r$ (protector does not fill all space among inequalities) for an inequality of 5 mm height is fulfilled for pressures in tire – road contact.

This effect could have influence on the sliding [16] and on the investigation of contact between tire and road as well in the aspect of noise [17] and safety [18].

Protector rigidity values of separate models are presented in Fig. 18. The model evaluating interaction with road texture (r = 5 mm) prescribes less stiffness values, but dependence $C - R_z$ remains similar and is related with nonlinear $q - R_z$ dependence.

5. Conclusions

1. Factors, having the largest influence in the evaluation of stiffness of tire protector in radial direction, i.e. dependence of pressure of tire –road contact on radial loading and breaker and cord influence on radial deformation of the protector, were determined. Evaluation model of protector deformations has no essential influence and a simple model, evaluating filling coefficient of the protector pattern may be used.
2. Evaluation of deformations of ribbed part of the protector by filling coefficients of the protector pattern is adequate to the model of deformation of rubber prisms.
3. Numerical simulation and experiments has confirmed that deformations of the protector band constrict breaker and cord layers, therefore stiffness of the protector band in direction Z is evaluated with stiffness of the whole band in directions X and Y defined. When elasticity modulus of the rubber is $E_r = 6$ MPa, for a motorcar tire is obtained $E_{1z} = 27$ MPa.
4. While evaluating ring stiffness of the protector, nonlinear $\Delta\delta - R_z$ dependence has been obtained, so as due to tire deflection particularity dependence of relative pressure onto road q on radial loading is nonlinear.
5. It is recommended to evaluate protector stiffness of the tire in relative coordinates R_z / R_{znom}, because in this case the tire type has less influence.

References

1. **Bukhin, B.L.** 1988. Introduction into Mechanics of a Pneumatic Tire. Moskva: Khimia. 224p. (in Russian).
2. **Pakalnis, A.** 2000. Investigation of elasticity characteristics in a tyre ring model, Mechanika 3(23): 59-62.
3. **Bohm, F.** 1996. Dynamic rolling process of tires as layered structures, Mechanics of Composite Materials, vol.32, No6: 824-834.
4. **Kido, I.; Nakamura, A.; Hayashi, T.; Asai, M.** 1999.

Suspension vibration analysis for road noise using finite element model. Proc. Noise and Vibration Conference, Michigan, vol.2: 1053-1060.
5. **Vansauskas, V.; Bogdevičius, M.** 2009. Investigation into the stability of driving an automobile on the road pavement with ruts, Transport 2(24): 170-179.
6. **Rutka, A.; Sapragonas, J.** 2002. Investigation of car suspension model, Mechanika 1(33): 41-46.
7. **Rutka, A.; Sapragonas, J.** 2002. The role of a tire in vehicle and road interaction, Transport, vol.17, №2: 39-45.
8. Calculation of the Strength in Mechanical Engineering. / S.D. Ponomarev, V.L. Biderman, K.K. Likharev, V.M. Makushin, N.N. Malinin, Knoroz. V.I. Feodosjev. Moskva, 1958, T2, 975p (in Russian).
9. **Gay, D.** 1997. Matėriaux composites. Paris: Hermes. 672p.
10. Composite materials: Manual. / V.V. Vasiljev, V.D. Portasov, V.V. Bolotin, at al. Moskva: Mashinostrojenie, 1990. 512p. (in Russian).
11. **Partaukas, N.; Bareišis, J.** 2009. The stress state in two-layer hollow cylindrical bars, Mechanika 1(75): 5-12.
12. **Ragulskis, K.; Dabkevičius, A.; Kibirkštis, E.; Bivainis, V.; Miliūnas, V.; Ragulskis, L.** 2009. Investigation of vibrations of a multilayered polymeric film, Mechanika 6(80: 30-36.
13. **Dimaitis, M.** 2000. Modeling interaction between road and vehicle, Mechanika 4(24): 65-69.
14. **Sapragonas, J.; Ostasevicius, V.; Pilkauskas, K.; Staliulionis, D.** 2002. Active car suspension with pneumatic muscle, Mechanika 5(37): 49-55.
15. **Matlin, M.; Kazankina, E.; Kazankin V.** 2009. Mechanics of initial dot contact, Mechanika 2(76): 20-23.
16. **Beneš, L.; Kaloč, R.; Minářm L.** 2010. A New approach to the analysis of the contact surfaces of rolling kinematic couple, Transport 4(25): 382-386.
17. **Leipus, L.; Butkus, D.; Januševičius, T.** 2010. Research on motor transport produced noise on gravel and asphalt roads, The Baltic Journal of Road and Bridge Engineering, vol.V, No 3: 125-131.
18. **Laurinavičius, A.; Skerys, K.; Jasiūnienė, V.; Pakalnis, A.; Starevičius, M.** 2009. Analysis and evaluation of the effect of studded tyres on road pavement and environment (I), The Baltic Journal of Road and Bridge Engineering, vol.IV, No 3: 115-122.

J. Sapragonas, A. Dargužis

AUTOMOBILIO PADANGOS PROTEKTORIAUS RADIALINIŲ DEFORMACIJŲ MODELIS

R e z i u m ė

Straipsnyje pateikiami rezultatai skaitinio ir eksperimentinio tyrimo, kuriuo siekiama nustatyti padangos protektoriaus, kaip atskiro elemento pakabos dinaminiuose modeliuose, standumą. Skaitiniu modeliavimu nustatyta, kad rantytosios dalies aprašymas, įvertinant rašto užpildymo koeficientą, adekvatus guminių prizmių deformavimo modeliams. Bandymai patvirtino, kad sudarant skaitinius modelius būtina įvertinti protektoriaus deformacijos suvaržymą standžiais brekerio ir kordo sluoksniais, dėl kurio radialinė protektoriaus deformacija sumažėja 1.7 - 2.1 karto. Deformacijos ir apkrovos tarpusavio priklausomybė kontakto paviršiaus nelygumo įvertinimo kokybiškai nepakeičia. Tiksliau įvertinus protektoriaus darbo sąlygas sluoksnio rezultatai sutampa su bandymo rezultatais.

J. Sapragonas, A. Darguzis

MODEL OF RADIAL DEFORMATIONS OF PROTECTOR OF VEHICLE TIRE

S u m m a r y

Numerical and experimental investigation results in order to find out stiffness of the tire protector, as single element in dynamic models of a suspension are presented in this paper. Numerical modeling demonstrated that description of ribbed part with the evaluation of pattern filling coefficient was adequate to rubber prisms deformation models. Testing confirmed that in numerical models it was necessary to evaluate constriction of protector's deformation by rigid breaker and cord layers, that is why radial deformation of the protector decreases 1.7 - 2.1 times. Taking into account unevenness of contact surface stiffness–loading dependence does not bring qualitative changes. With more correct evaluation of operational conditions of the protector layer results coincide with testing results.

Й. Сапрагонас, А. Даргужис

МОДЕЛЬ РАДИАЛЬНЫХ ДЕФОРМАЦИЙ АВТОМОБИЛЬНОЙ ШИНЫ

Р е з ю м е

В статье представлены результаты численного моделирования и экспериментального исследования с целью установить жесткость протектора шины, как отдельного элемента в динамических моделях подвески. С помощью численного моделирования установлено, что описание жесткости части протектора с рисунком с учетом коэффициента наполнения узора адекватен деформационным моделям резиновых призм. Испытаниями подтверждено, что в численных моделях необходимо учесть ограничение деформации протектора жесткими слоями брекера и корда, из-за чего радиальная деформация протектора становится меньше на 1.7 - 2.1 раза. Оценка неровностей контактной поверхности качественных изменений зависимости жесткость - нагрузка не вносит. Оценивая рабочие условия более точно, результаты жесткости слоя совпадают с результатами испытаний.

Received October 04, 2010
Accepted January 28, 2011